nature climate change

SUPPLEMENTARY INFORMATION

DOI: 10.1038/NCLIMATE3220

In the format provided by the authors and unedited.

Aerosol-weakened summer monsoons decrease lake fertilization on the Chinese Loess Plateau

Jianbao Liu[1,2], Kathleen M. Rühland[3], Jianhui Chen[1], Yangyang Xu[4], Shengqian Chen[1], Qiaomei Chen[1], Wei Huang[1], Qinghai Xu[5], Fahu Chen[1,2]* and John P. Smol[3]*

[1]Key Laboratory of West China's Environmental System (Ministry of Education), College of Earth and Environmental Sciences, Lanzhou University, Lanzhou 730000, China. [2]CAS Center for Excellence in Tibetan Plateau Earth Sciences of the Chinese Academy of Sciences, Beijing 100101, China. [3]Paleoecological Environmental Assessment and Research Lab (PEARL), Department of Biology, Queen's University, Kingston, Ontario, K7L 3N6, Canada. [4]Department of Atmospheric Science, Texas A&M University, College Station, Texas 77842, USA. [5]Institute of Nihewan Archaeology Research College of Resources and Environment, Hebei Normal University, Shijiazhuang 050024, China. *e-mail: fhchen@lzu.edu.cn; smolj@queensu.ca

16 **Supplementary Figures**

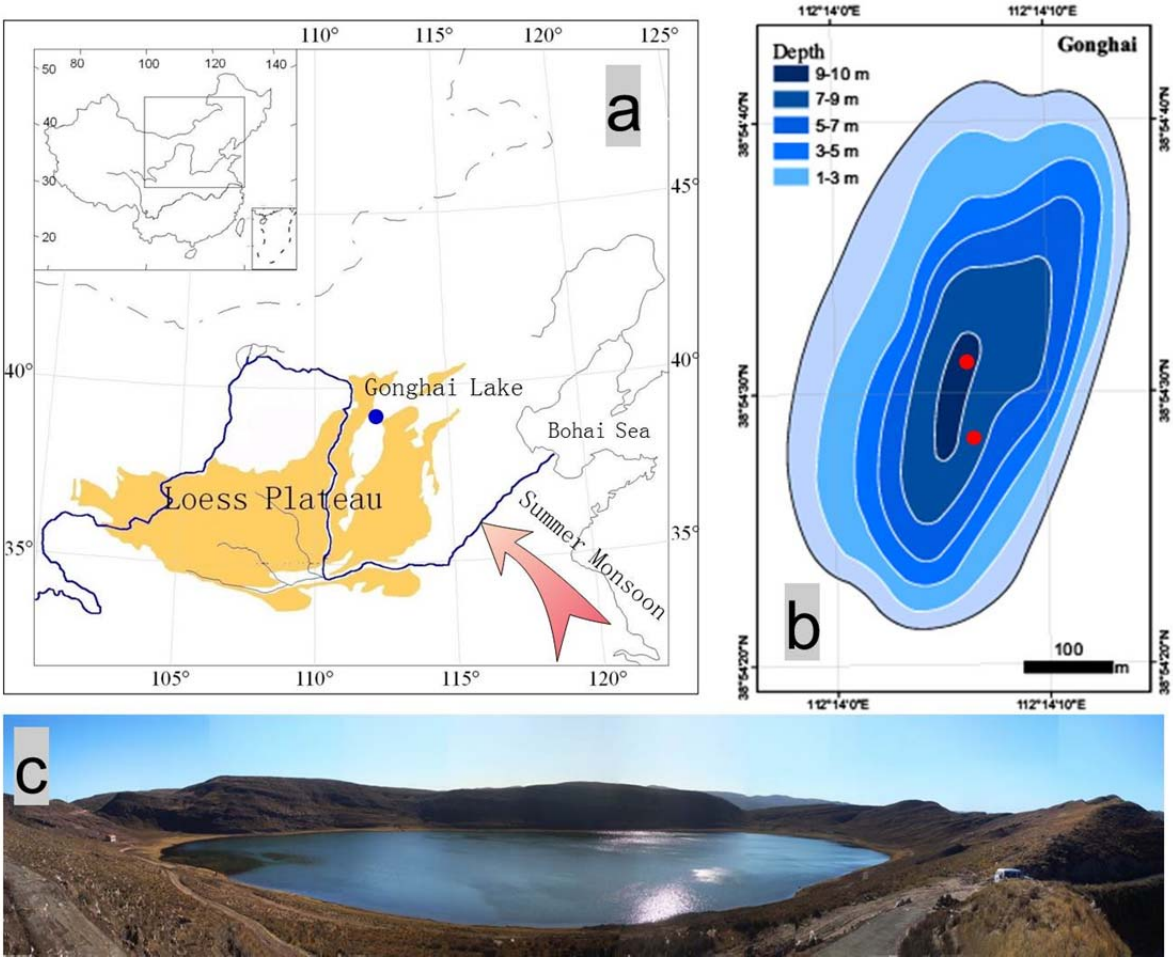

17

18 **Figure S1 | Location and settings.** (**a**) Location of Lake Gonghai (blue circle) in the Chinese
19 Loess Plateau. The Yellow River (blue line) and the dominant circulation system (arrows) of the
20 Asia summer monsoon are also shown. (**b**) Bathymetry of Lake Gonghai. The red dots indicate
21 the location of the Lake Gonghai sediment cores. (**c**) Photograph of Lake Gonghai and its
22 catchment.

23

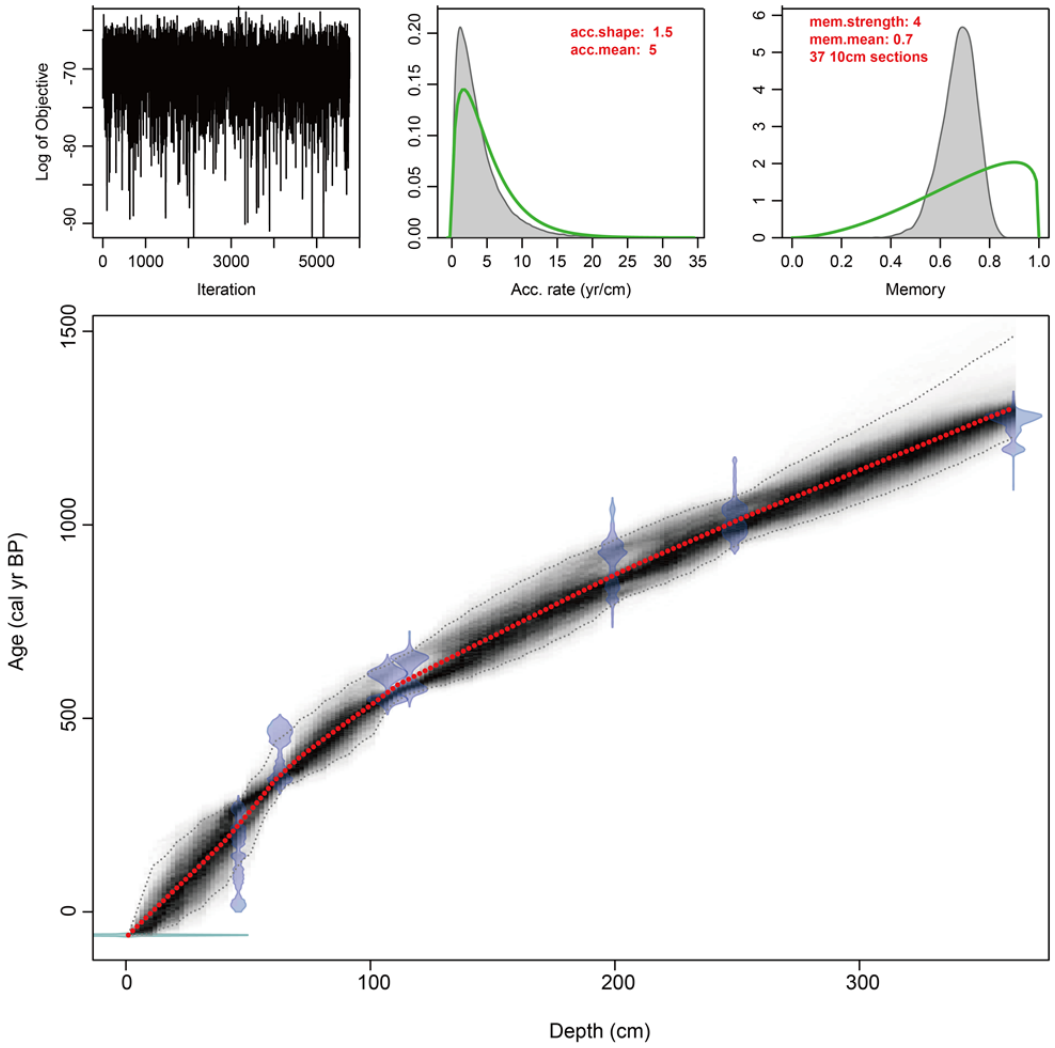

Figure S2 | Age-depth model for the Lake Gonghai sediment core (GH09B) over the past 2000 years. Upper panels depict the Markov Chain Monte Carlo (MCMC) iterations (left; good runs show a stationary distribution with little structure among neighbouring iterations), the prior (green curves) and posterior (grey histograms) distributions for the accumulation rate (middle panel) and memory (right panel). The bottom panel shows the calibrated ^{14}C dates (transparent light blue) and the age-depth model (darker greys indicate most probable calendar ages; grey stippled lines represent 95% confidence intervals; red curve shows single 'best' model based on the weighted mean age for each depth interval).

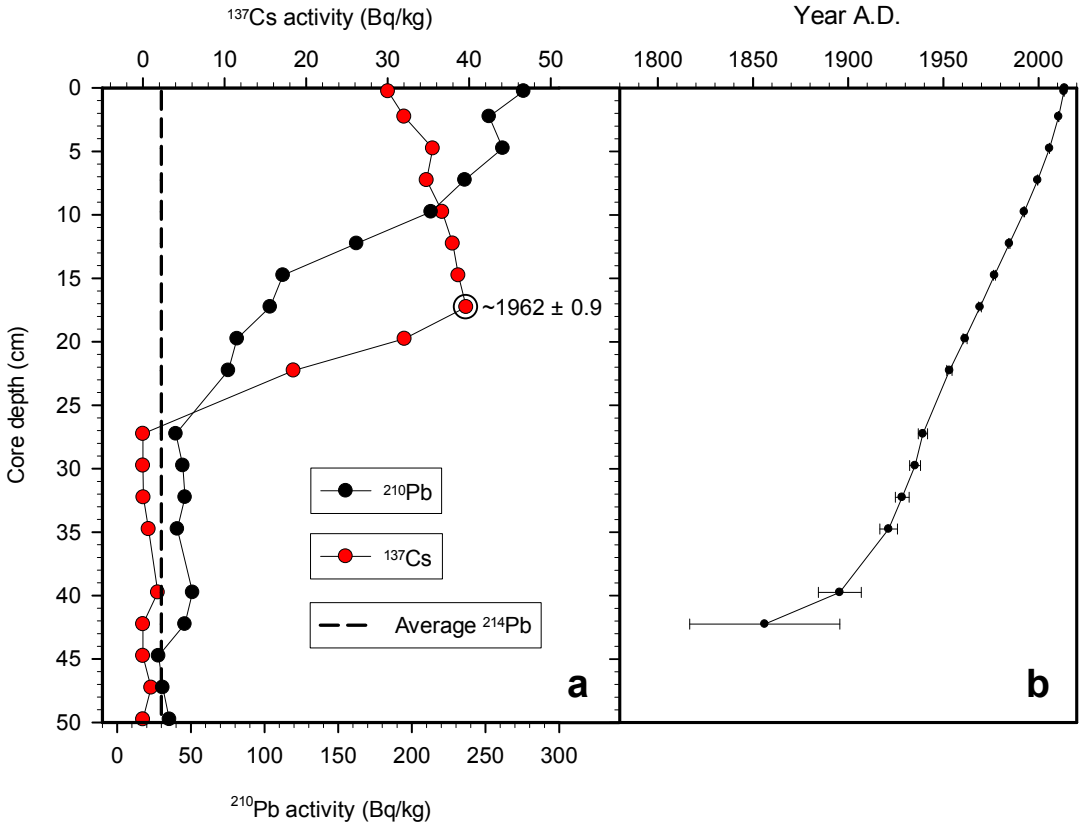

Figure S3 | Age-depth model for the Lake Gonghai surface sediment core (GH13F) over the past ~150 years. Radiometric dating analysis using gamma spectroscopy showing (**a**) ^{210}Pb, ^{214}Pb, and ^{137}Cs activities in becquerels per kilogram (Bq/kg) dried sediment plotted against core depth, and (**b**) estimated age (A.D.) plotted against core depth and associated errors based on the constant rate of supply (CRS) model. The dashed vertical line in (a) is the mean of all sample-specific ^{214}Pb activities counted in the core and is a proxy for supported ^{210}Pb. The CRS date of 1962 ± 0.9 associated with the interval of highest ^{137}Cs activity depicted in (**a**) is an excellent match with the height of nuclear fallout resulting from the 1963 global moratorium on weapons testing, further confirming the veracity of the ^{210}Pb dating chronology.

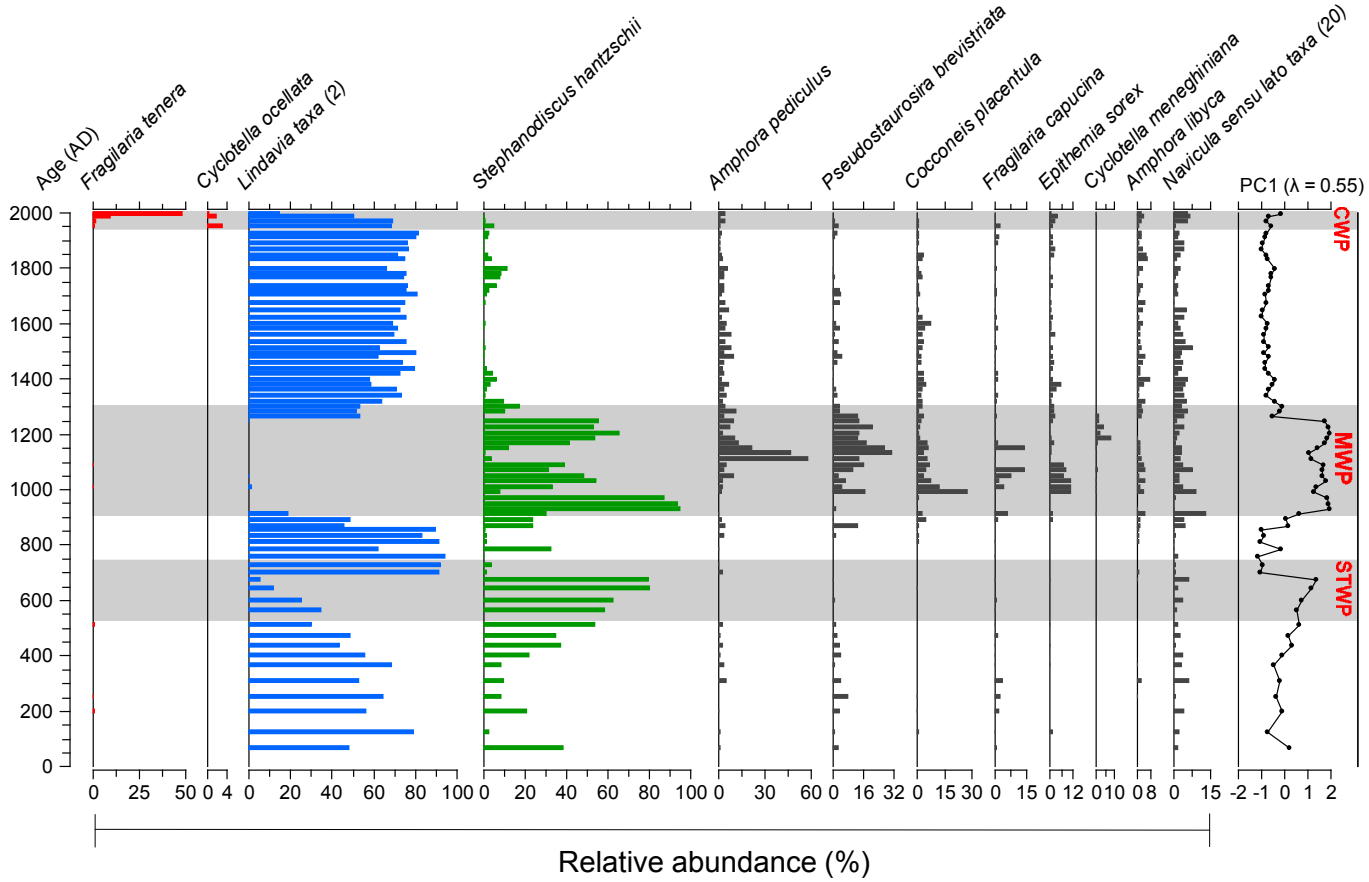

Figure S4 | Stratigraphic profile showing the relative abundances of the most common diatom taxa from Lake Gonghai (core GH09B), as well as the PCA axis 1 sample scores of the diatom assemblages. Some diatom taxa have been grouped for clarity and the number of taxa in each group is indicated in parentheses. The dominant oligotrophic *Lindavia* taxa (*L. praetermissa and L. bodanica*) and eutrophic *Stephanodiscus hantzschii* are presented in blue and green, respectively. The shaded areas represent the Sui-Tang Warm Period (STWP), the Medieval Warm Period (MWP), and the Current Warm Period (CWP). Cluster analysis using constrained incremental sum of squares (CONISS) with Euclidean squared distances as the measure of dissimilarity generated in TGView v. 1.7.16[1] determined that stratigraphic zones (dendrogram not shown) matched the timing of high magnitude diatom responses to the three warm periods. λ represents the associated eigenvalue for the PCA axis 1 sample scores.

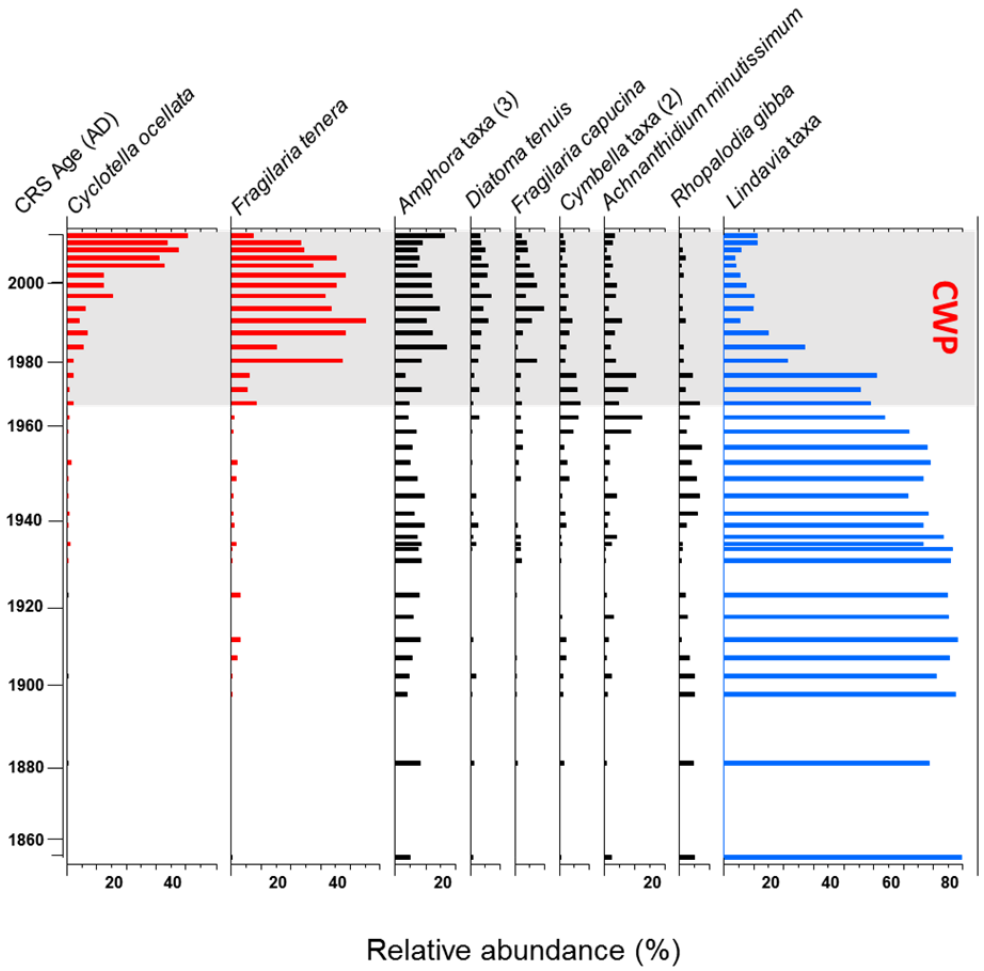

Figure S5 | Stratigraphic profile showing the percent relative abundances of the most common diatom taxa (occurring at 5% in at least 4 intervals) from the Lake Gonghai short core (GH13F). Certain genera were grouped for clarity and the number of taxa in each group are indicated in parentheses (e.g. *Amphora* and *Cymbella*). The shaded area represents a pronounced increase in regional and global mean air temperature during the Current Warm Period (CWP). Cluster analysis using constrained incremental sum of squares (CONISS) with Euclidean squared distances as the measure of dissimilarity generated in TGView v. 1.7.16[1] determined that the main stratigraphic zones (dendrogram not shown) matched the timing of high magnitude diatom responses during the CWP.

Supplementary Table

Table S1 Radiocarbon dates of terrestrial plant-macrofossil samples used to construct the chronology for core GH09B from Lake Gonghai.

Lab ID	Sample No.	Depth (cm)	Material	$\delta^{13}C$ ‰	Conventional Age (1σ, BP yr)	Calibrated Age(1σ, Cal yr BP)
Beta306751	GHB1-35	46	Stem	-25.9	150±30	0-282
XA4667	GHB1-48	63	Leaf	-24.9	368±23	332-498
XA5587	GHB1-82	107	Leaf	-15.7	570±25	540-628
XA4669	GHB1-89	116	Stem	-30.7	665±34	565-668
XA4670	GHB1-153	199	Stem	-30.9	1005±40	804-963
XA4668	GHB1-191	249	Stem	-30.4	1102±30	968-1053
XA4671	GHB2-76	363	Stem	-25.4	1329±25	1194-1294

References

1. Grimm, E. C. CONISS: a Fortran 77 program for stratigraphically constrained cluster analysis by the method of incremental sum of squares. *Comput. Geosci.* **13**, 13–35 (1987).